Review and test of methods for determination of the Schottky diode parameters

O. Ya. Olikh[1, a)]
Faculty of Physics, Taras Shevchenko National University of Kyiv, Kyiv 01601, Ukraine

(Dated: 31 March 2015)

This paper deals with the extraction of the Schottky diode parameters from a current-voltage characteristic. 10 analytical methods, 2 numerical methods, and 4 evolutionary algorithms of the series resistance, barrier height, and ideality factor determination are reviewed. The accuracy of the methods is quantified using a wide range of both ideal and noisy synthetic data. In addition, the influencing factors of the parameters extraction accuracy are estimated. The adaptive procedure, which improves the precision of analytical Gromov's method, is suggested. The use of Lambert W function has been shown to reduce the error of parameter extraction by numerical method. Finally all methods are applied to experimental data. The most reliable and preferred methods are chosen.

PACS numbers: 73.30.+y

I. INTRODUCTION

The Schottky diode (SD) is one of the most commonly used semiconductor devices. It has advantages of low forward voltage drop, fast response and low resistance. SDs are widely applied in high-speed logic circuits, integrated and optoelectronic technologies, including microwave diodes field-effect transistors, various detectors, solar cells. Determining the SD parameters, which must be taken into account in practical application, plays an important role in the designing and manufacturing process.

The forward bias current-voltage (I–V) characteristics, according to the thermionic emission SD model, can be expressed as[1]

$$I = I_s \left\{ \exp\left[\frac{q(V - IR_s)}{nkT} \right] - 1 \right\} \tag{1}$$

$$I_s = AA^* T^2 \exp\left(-\frac{q\Phi_b}{kT} \right) \tag{2}$$

where I_s is the saturation current, q is the electron charge, R_s is the series resistance, n is the ideality factor, k is the Boltzmann constant, T is the absolute temperature, A is the diode area, A^* is the effective Richardson constant, Φ_b is zero bias Schottky barrier height (SBH). Φ_b (or I_s), n and R_s are the fundamental parameters of the SD model and should be determined as accurately as possible from experimental I–V characteristics.

Some authors have proposed different methods to determine the SDs parameters. The elementary standard method requires the presence of the linear region on the $\ln(I)$ vs V plot[1,2] and then two parameters Φ_b and n can be obtained from the plot intercept and slope respectively. Unfortunately, this simple analysis fails when an essential R_s is present. Altogether a series resistance presence complicates considerably a mathematical aspect of a parameters extraction and turns Eq. (1) into transcedental. Therefore the set of analytical methods has been proposed. These methods are characterized by a straightforward algebraic approach and use some auxiliary function,[3–11] the derivative[12] or integration[13–15] of current with respect to voltage, several I–V measurements at different temperatures[16] or with an external resistance.[17] On the other hand, the parameters extraction is a multidimensional numerical optimization problem and various numerical methods have been proposed in the literature.[18–21] These methods generally use gradient-descent techniques to minimize the difference in measured and fitting current values. Some authors[22,23] have utilized the Lambert W function to obtain solution of Eq. (1). Numerical methods are said to have an overall higher level of confidence in terms of the parameters resulting values, but may require a relatively long computation time and may tend to converge to local rather than global extremum. Several summary of methods is given in the literature,[19,24] however they are focused mainly on a few methods only.

In addition, recently evolutionary algorithm (EA) techniques have been used to semiconductor devices parameter determination.[25–32] EA is a stochastic optimization method that appears to be very efficient in optimizing real-valued multi-modal objective functions. In contrast to numerical methods, EA is able to handle nonlinear functions without requiring derivatives information and depends weakly on a starting values of the parameters that are introduced prior to the algorithm running. EA is considered[28] to be more promising than other computational methods.

Our goal is to compare the accuracy and running time of different methods of SD parameters extraction. In this work, we restrict ourselves to methods which use a single I–V curve and focus on 10 analytical methods, 2 numerical methods (the least-squares (LS) curve fitting by using

a) Electronic mail: olikh@univ.kiev.ua

both Eq. (1) directly and Eq. (1) solution expressed in Lambert function terms) and 4 evolutionary algorithms (the penalty based differential evolution (DE), the particle swarm optimization (PSO), the modified artificial bee colony (MABC) and the teaching learning based optimization (TLBO)). Firstly, the methods essence is described shortly. Then methods are examined on ideal synthetic I–V characteristics, on noisy synthetic data, and on experimental data; the different method results are compared. Finally conclusions are presented.

II. DATA PREPARATION

A. Experimental data

The Mo/n–n^+–Si structure was used to obtain experimental data. The samples were 0.2 μm thick n–Si:P epitaxial layer on 250 μm thick n^+–Si:Sb substrate. The square of molybdenum Schottky contact fabricated on the epi-layer surface was $A = 3.14 \cdot 10^{-6}$ m^2. The I–V characteristics were measured in the temperature range from 170 to 330 K.

B. Synthetic data

The silicon Schottky diode was assumed when data were synthesizing. The I–V characteristics were calculated by considering Eq. (1) using the bisection method. The values of $A = 3.14 \cdot 10^{-6}$ m^2 and of $A^* = 112$ A cm^{-2}K^{-2} (the n–Si case[33]) were chose. The voltage step was 0.01 V and the current varied from 10^{-9} to 10^{-1} A.

We wanted to test methods at various values of parameters and thereto data were generated in the temperature range from 130 to 330 K. At the same time we try to synthesize data, which are close to real diode. The temperature dependences of Φ_b, n and R_s were selected for following reasons. It is predicted theoretically[1] and observed experimentally[34,35], that, in the case of homogeneous Schottky contact, the SBH decreases with temperature increase in the way similar to semiconductor band gap. Therefore the Varshni equation[36] can be used to fit the SBH temperature dependence

$$\Phi_b(T) = \Phi_b(0) - 7.021 \cdot 10^{-4} T^2/(T + 1108), \quad (3)$$

where zero temperature SBH $\Phi_b(0)$ was chosen of 0.75 eV. The temperature dependence of the ideality factor is often described as follows

$$n = 1 + T_0/T, \quad (4)$$

where T_0 is within $20 \div 50$ K to silicon case.[34,37–39] The value of $T_0 = 35$ K was used when data were synthesizing. The temperature dependence of the series resistance can be described by the equation[2,40,41]

$$R_s = R_{s0} \exp(E_a/kT), \quad (5)$$

where E_a is the dopant activation energy. The values of $E_a = 0.44$ eV (the phosphorus impurity case) and $R_{s0} = 0.25$ Ω were used.

As a result the set of I–V data was composed of 21 curves, which were synthesized at 10 K intervals from 130 to 330 K; in this case Φ_b, n and R_s varied from 0.740 to 0.697 eV, from 1.27 to 1.11 and from 12.6 to 1.2 Ω respectively.

To take into account the probable random errors during measurements the another sets of I–V data (the noisy synthetic data) were generated too. In this case the voltage V_i and the current I_i of each $i-$th point of a I–V characteristic were random values with Gaussian distribution. The voltage mean value $\overline{V}_i$ varied with a step 0.01 V, the current mean value $\overline{I}_i$ was calculated by using Eq. (1) and $\overline{V}_i$. The voltage standard deviation σ_V was a fixed in a I–V data set. The current standard deviation σ_I depended on the current value $\sigma_I = \sigma_I^\varepsilon \cdot \overline{I}_i$, where constant σ_I^ε was an relative current standard deviation. Thus the different sets of synthetic I–V data were characterized by different σ_V and σ_I^ε values; the ideal synthetic characteristics were defined by $\sigma_V = 0$ V and $\sigma_I^\varepsilon = 0$.

The following variables are used to evaluate the accuracy of every method. The precision of the ideality factor extraction from a single I–V curve χ_n^q is estimated by

$$\chi_n^q = \left(\frac{n_{ext} - n_{ac}}{n_{ac}} \right)^2, \quad (6)$$

where n_{ext} is the parameter extraction result, n_{ac} is the accurate value, which used during data synthesizing.

The precision of the n determination from a I–V data set ε_n is calculated by

$$\varepsilon_n = \sqrt[2N_{IV}]{\prod_{i=1}^{N_{IV}} \chi_{n,i}^q}, \quad (7)$$

where N_{IV} is the total number of I–V characteristics in the set. Notably ε_n is square root of χ_n^q geometric mean. The variables, which used to estimate the SBH and series resistance determination from a single I–V curve χ_Φ^q and χ_R^q and from a I–V characteristic set ε_Φ and ε_R, are calculated similarly to Eqs. (6) and (7).

III. USED METHODS

A. Analytical methods

1. Norde method

The modified Norde method[3,4,16,42] bases on an auxiliary function:

$$F(V) = \frac{V}{\gamma} - \frac{kT}{q} \ln \left(\frac{I(V)}{AA^*T^2} \right), \quad (8)$$

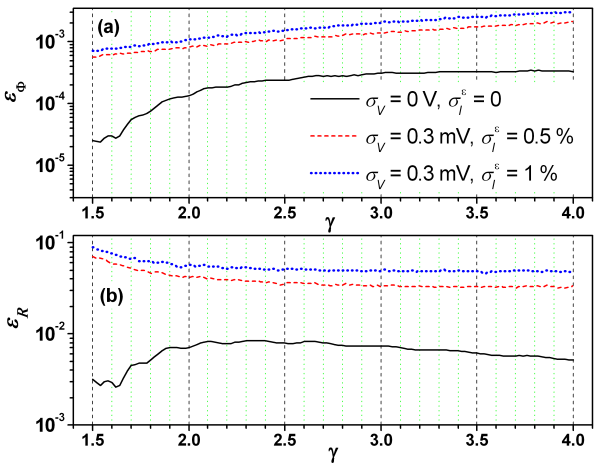

FIG. 1. Dependences of the Φ_b (a) and R_s (b) determination accuracy on γ. Norde method is applied to sets of ideal synthetic data (solid line) and noisy synthetic data (dotted and dashed lines).

where γ is an arbitrary constant greater than the ideality factor. The SBH and series resistance values can be determined as

$$\Phi_b = F(V_{min}) + \frac{\gamma - n}{n}\left(\frac{V_{min}}{\gamma} - \frac{kT}{q}\right), \tag{9}$$

$$R_s = \frac{(\gamma - n)kT}{qI_{min}}, \tag{10}$$

where $F(V_{min})$ and V_{min} are the coordinates of minimum point in the plot $F(V)$ vs V; I_{min} is the current value at the voltage V_{min}.

What we want to stress is that the n value is necessary for the Norde method. As a result, n_{ac} and value, which has been determined by MABC method, were used during Norde method application to synthetic and experimental data respectively.

It should be noted that Norde's function minimum was not observed in the case of a conventional synthetic characteristics with $R_s < 5\ \Omega$. To occur function minimum for the whole set of plot $F(V)$ vs V the synthetic characteristics, which generated up to 10^{-1} A, were used in the Norde and Bohlin (see below) methods.

The Norde method accuracy dependence on γ value was calculated — see Fig. 1. The value $\gamma = 1.8$ was used to minimize the method error.

2. Werner method

Werner[5] showed, that for $V_d = (V - IR_s) \gg nkT/q$:

$$\frac{(dI/dV)}{I} = \frac{q}{nkT}\left[1 - R_s\left(\frac{dI}{dV}\right)\right]. \tag{11}$$

Eq. (11) shows that a plot of $(dI/dV)/I$ vs (dI/dV) yields a straight line that leads to R_s and n.

Unfortunately, this method is enable to determinate two parameters only. We proceed to evaluate the SBH as follow. For estimated R_s value, the experimental or synthetic curve $\ln I$ vs V was corrected and became $\ln I$ vs V_d. Then, a linear least-square fitting was made over a voltage range $V_d > 3kT/q$. It should be noted that during last fitting the slope can be considered as an independent variable or as the known quantity, which is defined by previously estimated n. Both cases were under consideration by us. If R_s and n have been estimated with help Eq. (11) and Φ_b has been deduced from the intercept of plot $\ln I$ vs V_d under known slope condition, then the marking "Werner method" was used. If R_s has been estimated with help Eq. (11) and then Φ_b and n have been deduced from the plot $\ln I$ vs V_d, then the marking "Werner* method" was used. The similar notations were used for other methods too.

3. Cibils method

Cibils and Buitrago[10] proposed to use an auxiliary function

$$F_a(V) = V - V_a \ln I, \tag{12}$$

where V_a is an arbitrary voltage, $V_a \geq 99.5 I_s R_s + nkT/q$. If $I_{min,a}$ is the current value at the voltage V_{min} where the function $F_a(V)$ exhibits a minimum, than the plot of $I_{min,a}$ vs V_a is expected[10] to be linear:

$$I_{min,a} = (V_a - nkT/q)/R_s\,. \tag{13}$$

We used V_a in the range from 0.035 V to the I–V curve ultimate value; the V_a step was 1 mV.

4. Kaminski I method

Kaminski *et al.*[13] proposed two methods. According to the first one, the coordinates of $j-$th point of auxiliary plot are calculated by

$$Y_j = \frac{1}{I_j - I_1}\int_{V_1}^{V_j} I\,dV \quad \text{and} \quad X_j = \frac{I_j + I_1}{2}, \tag{14}$$

where V_i and I_i are the coordinates of $i-$th point of the I–V curve, $i \in (1, \ldots, N_p)$, $j \in (2, \ldots, N_p)$. The plot of Y vs X is expected[13] to be linear:

$$Y = nkT/q + R_s X \tag{15}$$

and the linear fitting permits to estimate R_s and n. The trapezoid method of numerical integration was used.

5. Kaminski II method

Second method[13] based on the plot of Y vs X, where

$$Y_k = \frac{\ln(I_j/I_i)}{I_j - I_i} \quad \text{and} \quad X_k = \frac{V_j - V_i}{I_j - I_i}, \tag{16}$$

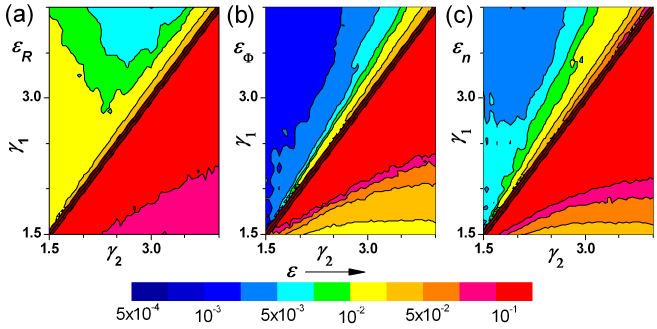

FIG. 2. Dependences of the R_s (a), Φ_b (b) and n (c) determination accuracy on γ_1 and γ_2. Bohlin method is applied to sets of synthetic data with $\sigma_V = 0$ V, $\sigma_I^\varepsilon = 0$ ($\gamma_1 > \gamma_2$ region) and $\sigma_V = 0.3$ mV, $\sigma_I^\varepsilon = 1\%$ ($\gamma_2 > \gamma_1$ region).

$i \in (1, \ldots, N_p - 1)$, $j \in (i+1, \ldots, N_p)$, $k \in (1, \ldots, N_p(N_p-1)/2)$. Used notations are similar to the previous subsection. The plot of Y vs X should follow a straight line[13]:

$$Y = q(-R_s + X)/nkT. \tag{17}$$

6. Bohlin method

Bohlin[9] used two different Norde's functions (two values of γ):

$$\begin{aligned} F_1(V) &= V/\gamma_1 - kT/q \cdot \ln(I/AA^*T^2), \\ F_2(V) &= V/\gamma_2 - kT/q \cdot \ln(I/AA^*T^2). \end{aligned} \tag{18}$$

The parameters are determined by

$$n = \frac{1}{2}\left[\frac{\gamma_1 I_{min,2} - \gamma_2 I_{min,1}}{I_{min,2} - I_{min,1}} + \frac{V_{min,1} - V_{min,2} + (\gamma_2 - \gamma_1)kT/q}{F_2(V_{min,2}) - F_1(V_{min,1}) - V_{min,2}/\gamma_2 + V_{min,1}/\gamma_1}\right], \tag{19}$$

$$Rs = \frac{kT}{2q}\left[\frac{\gamma_1 - n}{I_{min,1}} + \frac{\gamma_2 - n}{I_{min,2}}\right], \tag{20}$$

$$\Phi_b = \frac{1}{2}\left[F_1(V_{min,1}) + \frac{(\gamma_1 - n)(qV_{min,1} - \gamma_1 kT)}{\gamma_1 qn} + F_2(V_{min,2}) + \frac{(\gamma_2 - n)(qV_{min,2} - \gamma_2 kT)}{\gamma_2 qn}\right]. \tag{21}$$

where $[F_1(V_{min,1}), V_{min,1}]$ and $[F_2(V_{min,2}), V_{min,2}]$ are the coordinates of minimum points in the plots $F_1(V)$ vs V and $F_2(V)$ vs V respectively; $I_{min,1}$ and $I_{min,2}$ are the current values at the voltage $V_{min,1}$ and $V_{min,2}$ respectively.

The Bohlin method accuracy dependences on γ_1 and γ_2 values were calculated — see Fig. 2. The value $\gamma_1 = 1.6$ and $\gamma_2 = 3.5$ were used to minimize the method error.

7. Lee method

Suggested by Lee *et al.*[8], this method uses the functions array $\{F_L(I)\}$, where

$$F_L(I) = V(I) - V_a \ln I, \tag{22}$$

V_a is an arbitrary voltage. Each $F_L(I)$ function is approximated by

$$y(I) = c_1 + c_2 I + c_3 \ln I \tag{23}$$

and parameters c_1, c_2 and c_3 is determined. For $V > 3kT/q$, the dependence of $I_a = -c_3/c_2$ on V_a is expected[8] to be linear:

$$I_a(V_a) = (-nkT/q + V_a)/R_s. \tag{24}$$

The Φ_b can be calculated according to[8]

$$\Phi_b = c_3/n + kT/q \cdot \ln\left(AA^*T^2\right). \tag{25}$$

V_a was used in the range from 40 mV with 20 mV step; the $F_L(I)$ approximations were performed by the LS method.

8. Gromov method

Gromov and Pugachevich[7] proposed two methods. According to the first one, the plot of V vs I is fitted by Eq. (23) and

$$R_s = c_2\,, \tag{26}$$

$$n = (c_3 q)/(kT)\,, \tag{27}$$

$$\Phi_b = \left[c_1/c_3 + \ln\left(AA^*T^2\right)\right] kT/q\,. \tag{28}$$

According to the second method, the Eq. (23) approximation can be also applied to Norde's function with $\gamma = 2$:

$$F(I) = V(I)/2 - kT/q \cdot \ln(I/AA^*T^2). \tag{29}$$

In this case[7]

$$R_s = 2c_2\,, \tag{30}$$

$$n = (2c_3 q)/(kT) + 2\,, \tag{31}$$

$$\Phi_b = \frac{2c_1}{n} + \frac{(2-n)kT}{nq}\ln\left(AA^*T^2\right)\,. \tag{32}$$

The calculations have showed that two techniques produced same results.

The determination accuracy depends on a I—V curve range, which is used to auxiliary function construction — see Fig. 3. In this work, the special adaptive procedure was used. In this case, everything possible ranges were under consideration and parameters sets were determined. Then the value $\theta = \sum_{i=1}^{N_p}[1 - I_{calc}(V_i)/I_i]^2$ was calculated for every range. Here $I_{calc}(V_i)$ was calculated by using Eqs. (1–2) as well as determined parameters. Finally the parameters set, which satisfies minimum θ

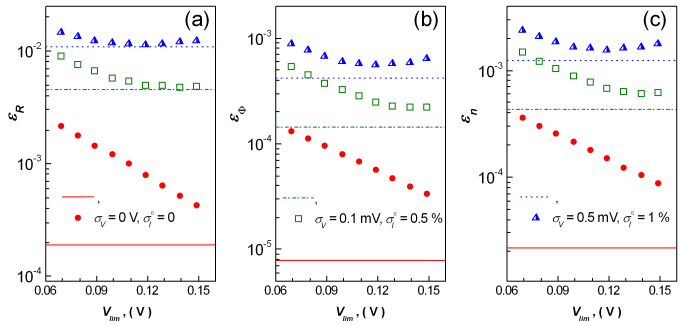

FIG. 3. Dependences of the R_s (a), Φ_b (b) and n (c) extraction accuracy for Gromov method. The points are calculated if the I—V curve range from V_{lim} to the ultimate voltage value is fitted by Eq. (23). The horizontal lines represent results, obtained by the adaptive procedure using.

value, was chosen. Fig. 3 shows, that the adaptive procedure allows to increase the precision of parameters determination.

If the adaptive procedure did not used then the Gromov method results were close to Lee method results. Therefore advantages of the proposed procedure can be determined hereinafter by the comparison of Gromov and Lee methods results.

9. Cheung method

Cheung and Cheung[6] derived the SD parameters from plots of $dV/d(\ln I)$ vs I and $H(V)$ vs I, where

$$H(I) = V - \frac{nkT}{q} \ln\left(\frac{I}{AA^*T^2}\right). \qquad (33)$$

If $V_d > 3kT/q$ then these plots are linear functions of the current

$$dV/d(\ln I) = R_s I + nkT/q, \qquad (34)$$

$$H(I) = n\Phi_b + IR_s. \qquad (35)$$

Initially R_s and n have been estimated by using Eq. (34), then Φ_b was estimated by using Eq. (35) and n value.

10. Mikhelashvili method

One of the techniques suggested by Mikhelashvili *et al.*[12] starts from the function $\alpha(V)$:

$$\alpha(V) = d(\ln I)/d(\ln V). \qquad (36)$$

The parameters value deduced by

$$R_s = \frac{V_{max}}{\alpha_{max}^2 I_{max}}, \qquad (37)$$

$$n = \frac{qV_{max}(\alpha_{max} - 1)}{\alpha_{max}^2 kT}, \qquad (38)$$

$$\Phi_b = \frac{kT}{q}\left[\alpha_{max} + 1 - \ln\left(\frac{I_{max}}{AA^*T^2}\right)\right]. \qquad (39)$$

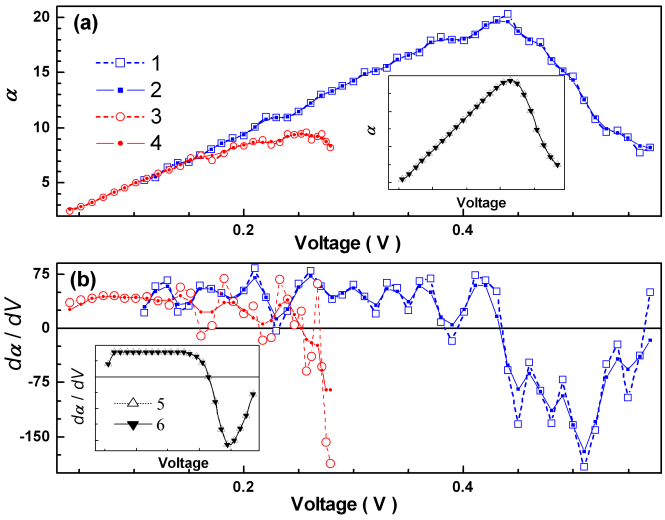

FIG. 4. The Mikhelashvili's curves (a) and theirs derivatives (b) as a function of voltage. The plots are performed for noisy synthetic data (1, 2, σ_V = 0.3 mV, σ_I^ε = 1%), for experimental data (3, 4) and for ideal synthetic data (5, 6, insets) before (1, 3, 5) and after (2, 4, 6) treatment.

where α_{max} and V_{max} are the coordinates of maximum point in the plot α vs V; I_{max} is the current value at the voltage V_{max}.

If experimental or noisy synthetic I—V curves are used then the numerical differentiation causes the appearance of the numerous local extremums in the α vs V plot. These extremums interfere to automatic determination of maximum point — see Fig. 4. Therefore the following special treatment was used. At first, the median 3-point filter has been applied to plot of α vs V; after that the 3-point smoothing was performed and afterwards a maximum point was determined.

B. Numerical methods

The standard method of least squares with statistical weights is used. Notably the parameters are determined by minimizing the sum of the vertical quadratic error:

$$S(I_s, n, R_s) = \sum_{i=1}^{N_p} I_i^{-1} \left[I_i - I_{calc}(V_i, I_s, n, R_s)\right]^2, \qquad (40)$$

where I_{calc} is the fitted values of the current. The system of non-linear equations is solved by the coordinate-wise gradient descent method. The criterion of the iterative procedure termination is $|\,(S_j - S_{j+1})/S_j\,| < 10^{-12}$, where S_j is the error sum at j—th iteration. The initial value of R_s is derived by the intercept of the plot of $(dV/dI)/I$ vs $1/I$, which is constructed by using 5 last points of the I–V data. The initial values of I_s and n are evaluated from the plot of $\ln I$ vs V, which is corrected by initial R_s value.

1. Ordinary LS method

In this case, I_{calc} was calculated by using Eq. (1).

2. Lambert LS method

The defining equation for the Lambert W function is $z = W(z) \cdot \exp(W(z))$. According to Jung and Guziewicz[22], an explisit solution of Eq. (1) can be given by using the basic branch of Lambert function:

$$I(V) = \frac{nkT}{qR_s} W\left\{\frac{qR_s}{nkT}\exp\left[\frac{q(V+R_sI_s)}{nkT}\right]\right\} + I_s. \quad (41)$$

Eq. (41) is correct if a shunt resistance is neglected. We calculated I_{calc} by using Eq. (41) in the Lambert LS method case.

C. Evolutionary algorithms

EAs are computational models that mimic natural evolution in their design and implementation. They work on a population P of candidate solutions $\overrightarrow{X}$: $P = \left\{\overrightarrow{X_k}\right\}$, $k \in (1, \ldots, N_S)$, where N_S is the number of solutions in the population. These candidate solutions are N_D–dimensional real-valued parameter vectors: $\overrightarrow{X_k} = \{x_{k,i}\}$, $i \in (1, \ldots, N_D)$, where N_D is the number of optimization parameters. In this work, $N_D = 3$, $\overrightarrow{X} = \{R_s, n, \ln I_s\}$.

In order to begin the optimization process, an initial population is created. Initial parameter values are usually randomly selected uniformly in the interval $[\overrightarrow{X}^L, \overrightarrow{X}^H]$:

$$x_{k,i,0} = x_i^L + r_{[0,1]}(x_i^H - x_i^L), \quad (42)$$

where $r_{[0,1]}$ is the random number distributed within the range $[0, 1]$, $\overrightarrow{X}^L = \left\{x_i^L\right\}$ and $\overrightarrow{X}^H = \left\{x_i^H\right\}$ are the lower and upper bound of the search space, respectively. In this work, the search ranges are set as follows $R_s \in [0, 50]$ Ω, $n \in [1, 2]$ and $I_s \in [10^{-26}, 10^{-2}]$ A.

At every iteration, (1) the current solutions are transformed to the next-step solutions: $\left\{\overrightarrow{X_{k,j-1}}\right\} \rightarrow \left\{\overrightarrow{X_{k,j}}\right\}$, $j \in (1, \ldots, N_{it})$, N_{it} is the maximum number of iterations; the transformation procedure depends on used algorithm and is described below; (2) the fitness function values $Fit(\overrightarrow{X_{k,j}})$ are calculated for each k-th solution. The optimal solution of j-th iteration $\overrightarrow{X}_j^{opt}$ is defined by minimum fitness function value: $Fit(\overrightarrow{X}_j^{opt}) = min\left\{Fit(\overrightarrow{X_{k,j}})\right\}$. The result of extraction is $\overrightarrow{X}_{N_{it}}^{opt}$.

In this paper, the fitness function can be given by

$$Fit = \sum_{i=1}^{N_p}\left\{1 - \frac{I_s}{I_i}\left[\exp\left(\frac{q(V_i - I_iR_s)}{nkT}\right) - 1\right]\right\}^2. \quad (43)$$

N_{it} depends on an attainment of solution convergence.

1. DE method

The differential evolution based on the theory of biological evolution. The solutions are called individual and the operators of j-th iteration are following[26]:

- Mutation. For each vector $\overrightarrow{X_{k,j-1}}$, a mutant vector $\overrightarrow{M_{k,j}}$ is generated according to

$$\overrightarrow{M_{k,j}} = \overrightarrow{X_{r_1,j-1}} + F_{sc} \cdot \left(\overrightarrow{X_{r_2,j-1}} - \overrightarrow{X_{r_3,j-1}}\right), \quad (44)$$

  where $r_1, r_2, r_3 \in (1, \ldots, N_S)$ are chosen randomly and are different from the running index k. $F_{sc} \in [0, 2]$ is a real and constant factor called scaling factor.

- Crossover. The trial vector $\overrightarrow{U_{k,j}}$ with

$$u_{k,i,j} = \begin{cases} m_{k,i,j}, & \text{if} \quad r_{[0,1]} \le CR \quad \text{or} \quad i = r_4 \\ x_{k,i,j-1}, & \text{otherwise} \end{cases} \quad (45)$$

  is formed; random $r_4 \in (1, \ldots, N_D)$ ensures that $\overrightarrow{U_{k,j}}$ obtains at least one element from $\overrightarrow{M_{k,j}}$; $CR \in [0, 1]$ is the crossover rate. According to Ishaque *et al.*[28], a penalty function can be used to avoid the solution from being stuck at the boundary. Any parameter that violates the limits is replaced with random values using

$$u_{k,i,j} = \begin{cases} u_{k,i,j} - r_{[0,1]}(x_i^H - x_i^L), & \text{if} \quad u_{k,i,j} > x_i^H \\ u_{k,i,j} + r_{[0,1]}(x_i^H - x_i^L), & \text{if} \quad u_{k,i,j} < x_i^L. \end{cases} \quad (46)$$

- Selection.

$$\overrightarrow{X_{k,j}} = \begin{cases} \overrightarrow{U_{k,j}}, & \text{if} \quad Fit(\overrightarrow{U_{k,j}}) < Fit(\overrightarrow{X_{k,j-1}}) \\ \overrightarrow{X_{k,j-1}}, & \text{otherwise.} \end{cases} \quad (47)$$

According to Wang and Ye[26], the values $F_{sc} = 0.8$, $CR = 0.3$ and $N_S = 8N_D = 24$ are used in this work. The convergence of the solution is attained at $N_{it} = 600$.

2. PSO method

The development of particle swarm optimization based on observations of the social behavior of animals such as bird flocking, fish schooling, and swarm theory. In a PSO algorithm, the solutions are called particles, which are flown or swum through hyperspace. The common operators of j-th iteration are described as follows[25]:

- The personal best of each particle $\overrightarrow{X_{k,j}}^{best}$ is determined:

$$\overrightarrow{X_{k,j}}^{best} = \begin{cases} \overrightarrow{X_{k,j-1}}^{best}, & \text{if} \quad Fit(\overrightarrow{X_{k,j-1}}) \ge Fit(\overrightarrow{X_{k,j-1}}^{best}) \\ \overrightarrow{X_{k,j-1}}, & \text{otherwise.} \end{cases} \quad (48)$$

- The global best to the position of the particle within the swarm $\overrightarrow{B}_j$ is identified:

$$\overrightarrow{B}_j = min\{Fit(\overrightarrow{X_{1,j}}^{best}), \ldots, Fit(\overrightarrow{X_{N_S,j}}^{best})\}. \quad (49)$$

- The velocity vector for each particle is changed according to

$$\upsilon_{k,i,j} = w_j\, \upsilon_{k,i,j-1} + l_1 r_{[0,1],1} \cdot (x^{best}_{k,i,j} - x_{k,i,j-1}) + l_2 r_{[0,1],2} \cdot (b_{i,j} - x_{k,i,j-1}), \quad (50)$$

where l_1 and l_2 are the learning factors, w_j is an inertia weight. In this investigation, the inertia weight is the following decreasing linear function:

$$w_j = w_{max} - j(w_{max} - w_{min})/N_{it}, \quad (51)$$

where w_{max} and w_{min} are the final weight and the initial weight, respectively. Then the velocity of each particle is updated according to the following relation:

$$\upsilon_{k,i,j} = \begin{cases} \upsilon_i^{max}, & \text{if} \quad \upsilon_{k,i,j} > \upsilon_i^{max} \\ -\upsilon_i^{max}, & \text{if} \quad \upsilon_{k,i,j} < -\upsilon_i^{max} \\ \upsilon_{k,i,j}, & \text{otherwise}, \end{cases} \quad (52)$$

where $\overrightarrow{\upsilon}^{max}$ is a constant in order to clamp the excessive roaming of particles. Generally, the choice of a $\overrightarrow{\upsilon}^{max}$ equals to the maximum allowable excursion of any particle in that dimension.[25]

- Each particle moved to its new position:

$$\overrightarrow{X_{k,j}} = \overrightarrow{\upsilon_{k,j}} + \overrightarrow{X_{k,j-1}}, \quad (53)$$

According to Ye *et al.*[25], the values $l_1 = l_2 = 2$, $w_{max} = 0.9$, $w_{min} = 0.4$ and $N_S = 15N_D = 45$ are used in this work. The initial velocity values $\overrightarrow{\upsilon_{k,0}} = 0$ are used. The convergence of the solution is attained at $N_{it} = 700$.

3. MABC method

The modified artificial bee colony algorithm based on the intelligent foraging behavior of honey bee swarm. The foraging honey bees are grouped into three categories; employed bees, onlookers and scout bees. The employed bees exploit their food sources and interact with onlooker bees. Onlooker bees wait in the hive and decide which food source to exploit. Scout bees carry out random searches for new food sources around the hive. The number of the employed bees or the onlooker bees is equal to the number of solutions. The position of a food source represents a possible solution to the optimization problem and the nectar amount of a food source is related to the fitness of the solution. When a food source is exploited fully by employed bee associated with it then, the food source is abandoned and bee becomes scout. The operators of j-th iteration are given below[30]:

- Produce a new solution $\overrightarrow{T_{k,j}}$ for each employed bee using

$$\overrightarrow{T_{k,j}} = \overrightarrow{X_{k,j-1}} + r_{[-1,1]}(\overrightarrow{X_{k,j-1}} - \overrightarrow{X_{r,j-1}}), \quad (54)$$

where $r \in (1, \ldots, N_S)$ is the randomly chosen index, $r \neq k$.

- Apply the greedy selection process for the employed bees:

$$\overrightarrow{X_{k,j-1}} = \begin{cases} \overrightarrow{T_{k,j}}, & \text{if } Fit(\overrightarrow{T_{k,j}}) < Fit(\overrightarrow{X_{k,j-1}}) \\ \overrightarrow{X_{k,j-1}}, & \text{otherwise.} \end{cases} \quad (55)$$

$$s_k = \begin{cases} 0, & \text{if } Fit(\overrightarrow{T_{k,j}}) < Fit(\overrightarrow{X_{k,j-1}}) \\ s_k + 1, & \text{otherwise.} \end{cases} \quad (56)$$

Here $\overrightarrow{S} = \{s_1, \ldots, s_{N_S}\}$ is the vector, which contain information related to the improvement of any of the food source during search. The initial values are $s_k = 0$.

- Calculate the probability p_k for each solutions:

$$p_k = \frac{(1 + Fit(\overrightarrow{X_{k,j-1}}))^{-1}}{\sum_{m=1}^{N_S}(1 + Fit(\overrightarrow{X_{m,j-1}}))^{-1}}. \quad (57)$$

- For each onlooker

(i) produce the new solutions $\overrightarrow{T_{k,j}}$ from the selected solution $\overrightarrow{X_{k,j-1}}$ by using Eq. (54) if $r_{[0,1]} < p_k$, $k = 1, \ldots, N_S$;

(ii) adopt the greedy selection mechanism — see Eqs. (55) and (56).

- Determine the abandoned solution for the scout, if exists, and replace it with a new randomly produced solution

$$x_{k,i,j} = \begin{cases} x_i^L + r_{[0,1]}(x_i^H - x_i^L) & \text{if} \quad s_k > L_{imit} \\ x_{k,i,j-1}, & \text{otherwise.} \end{cases} \quad (58)$$

where L_{imit} is the control parameters of the algorithm and it determines the number of allowable generations for which each non-improved food source is to be abandoned.

According to Karaboga *et al.*[30], the values $L_{imit} = 36$ and $N_S = 24$ are used in this work. In addition, it is considered, that the best solution can not be an abandoned solution. The convergence of the solution is attained at $N_{it} = 250$.

4. TLBO method

The teaching learning based optimization algorithm employs the concept of teaching–learning process in a classroom. A group of learners in the classroom is considered as population. The algorithm is inspired by passing on knowledge within a classroom environment, where

learners first obtain their knowledge from a teacher and then they also interact with each other. The common operators of j-th iteration are described as follows[25]:

- Teacher phase. The modified learner $\overrightarrow{T}_{k,j}$ is produced

$$\overrightarrow{T}_{k,j} = \overrightarrow{X}_{k,j-1} + r_{[0,1]} \left(\overrightarrow{X}^{opt}_{j-1} - r_{(1,\ldots,2)} \overrightarrow{X}^{mean}_{j-1} \right), \quad (59)$$

for each learner $(\overrightarrow{X}_{k,j-1})$ except teacher $(\overrightarrow{X}^{opt}_{j-1})$. Here

$$x^{mean}_{i,j-1} = \frac{1}{N_S} \sum_{k=1}^{N_S} x_{k,i,j-1}. \quad (60)$$

If $\overrightarrow{T}_{k,j}$ is found to be better than $\overrightarrow{X}_{k,j-1}$, it replaces $\overrightarrow{X}_{k,j-1}$ according to Eq. (55).

- Learner phase. For each learner, a new solution $\overrightarrow{U}_{k,j}$ is generated according to

$$\overrightarrow{U}_{k,j} = \overrightarrow{X}_{k,j-1} + r_{[0,1]} \left(\overrightarrow{X}_{k,j-1} - \overrightarrow{X}_{r,j-1} \right), \quad (61)$$
$$\text{if} \quad Fit(\overrightarrow{X}_{k,j-1}) > Fit(\overrightarrow{X}_{r,j-1})$$
$$\overrightarrow{U}_{k,j} = \overrightarrow{X}_{k,j-1} - r_{[0,1]} \left(\overrightarrow{X}_{k,j-1} - \overrightarrow{X}_{r,j-1} \right), \quad (62)$$
$$\text{if} \quad Fit(\overrightarrow{X}_{k,j-1}) \leq Fit(\overrightarrow{X}_{r,j-1}),$$

where $r \in (1, \ldots, N_S)$ is the randomly chosen index, $r \neq k$. Then $\overrightarrow{X}_{k,j}$ is determined according to Eq. (47).

In this work, the value $N_S = 1000$ is used and the convergence of the solution is attained at $N_{it} = 900$.

D. Running time of methods

Another criterion for electing the preferred method may be the elapsed running time (RT) of the parameters determination. RT is estimated by using WinAPI-functions $QueryPerformanceCounter()$ and $QueryPerformanceFrequency()$. The calculation was processed in a PC with the following features: AMD A4-3400 2.7 GHz CPU, 3072 MB RAM and a Windows XP OS. Obviously the precise extraction time depends on a program realization, a CPU workload and so on. Nevertheless all methods are tested under same conditions. So the used approach allows to obtain correlation of different methods RT and to estimate order of RT magnitude.

IV. RESULTS AND DISCUSSION

A. Parameter determination with ideal synthetic data

Firstly what we want to stress is that all evolutionary algorithms yield very similar parameters extraction

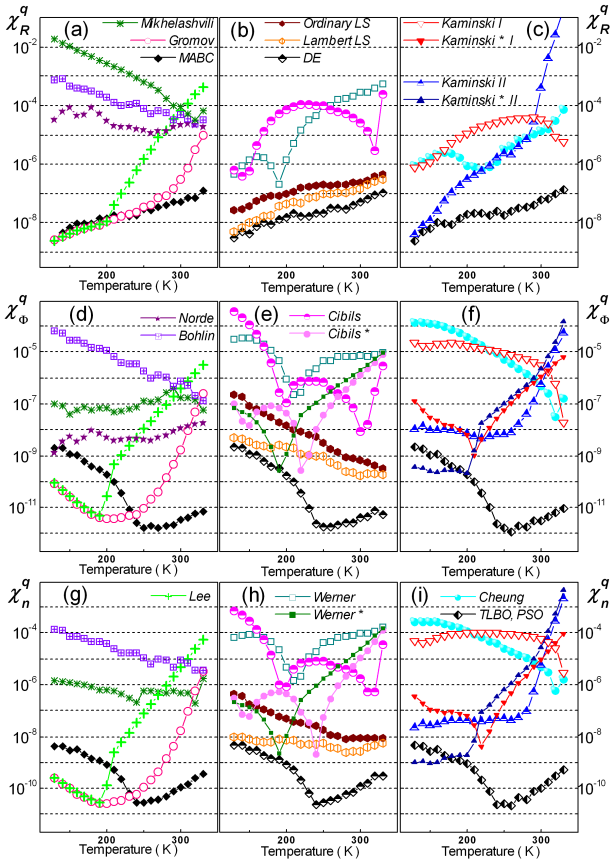

FIG. 5. Dependences of the precision of the series resistance (a – c), SBH (d – f) and ideality factor (g – i) determination by different methods on the synthesis temperature. The set of ideal synthetic I–V curves is used.

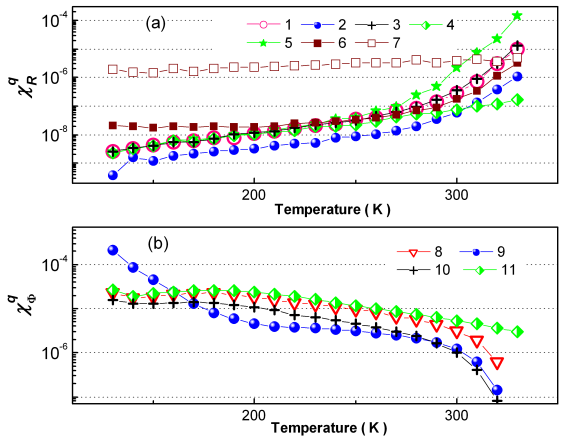

FIG. 6. Dependences of the precision of R_s (a) and Φ_b (b) extraction from a single curve by Gromov (a) and Kaminskii I (b) methods on the synthesis temperature. During sets synthesis, parameters were calculated by using Eqs. (2–5) mainly, but for curves 2 and 9 R_s was 3 times as large; for curves 3 and 10 n was 1.2 times as large; for curves 4 and 11 I_s was as 100 times as small; for curve 5 Φ_b was lowered by 0.1 eV; for curve 6 R_s and Φ_b were invariable and equal to 2 Ω and 0.7 eV; for curve 7 R_s and I_s were invariable and equal to 2 Ω and 10^{-5} A.

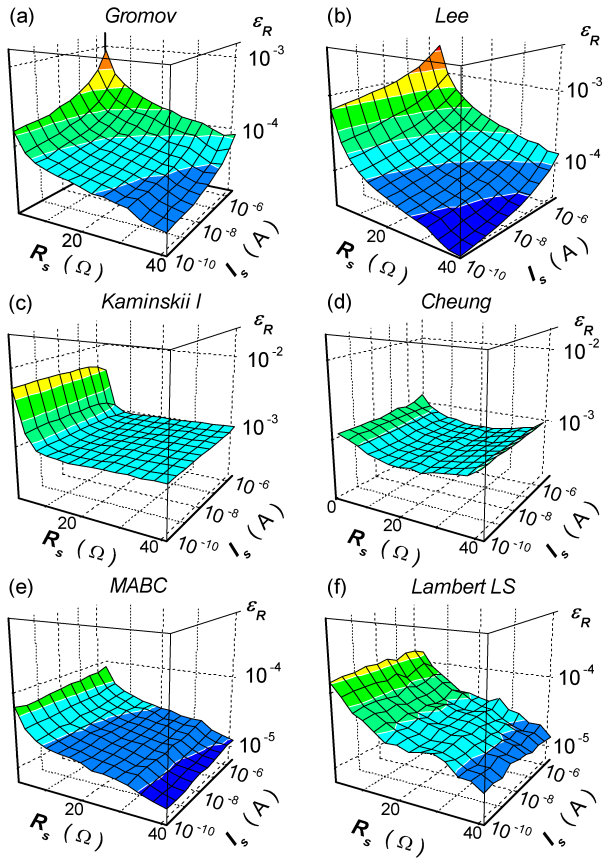

FIG. 7. Accuracy of the series resistance extraction from data sets, which calculated using invariable values of both R_s and I_s. The results of Gromov (a), Lee (b), Kaminskii I (c), Cheung (d), MABC (e), and Lambert LS (f) methods are shown.

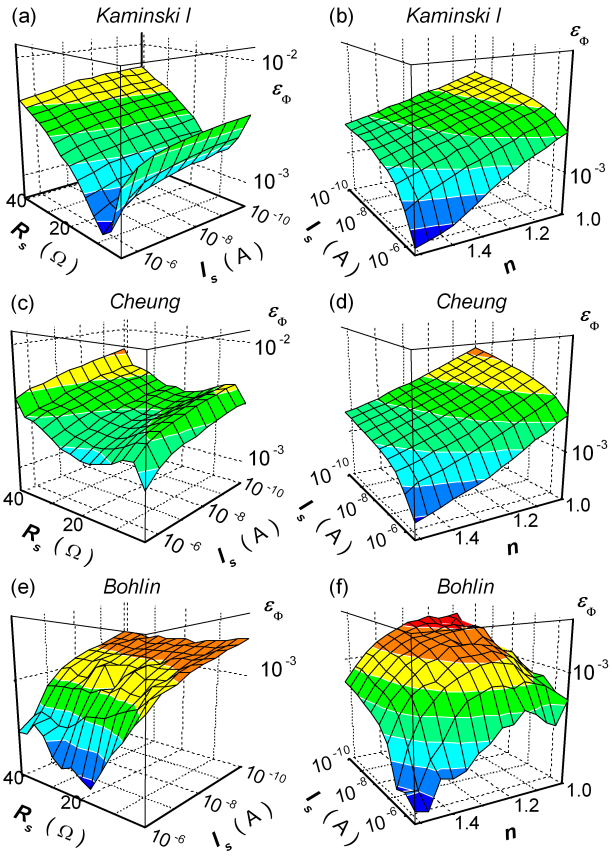

FIG. 8. Accuracy of the SBH extraction from data sets, which calculated using invariable value of both R_s and I_s (a, c, e) and invariable values of both n and I_s (b, d, f). The results of Kaminskii I (a, b), Cheung (c, d), and Bohlin (e, f) methods are shown.

results. It was expectedly because identical fitness function has been used.

The accuracy of the parameters extraction is shown on Fig. 5. One can see that the use of the adaptive procedure in Gromov method enables to considerably decrease the parameter determination error. The use of Lambert function for numerical calculation results the determination errors reduce. If Werner, Cibils, or Kaminskii I methods are applied then it is better to determine the R_s only with help an auxiliary function. After that, Φ_b and n can be determined by using a corrected I–V curve and a linear fitting. I.e., the asterisk-versions of these method are preferred. Finally, the evolutionary algorithms, Lambert LS, Norde (Φ_b determination), Ordinary LS (R_s determination), adaptive Gromov and Lee (except at hight temperature and I_s) methods yield the most accurate results from ideal I–V curves.

Precision is shown to vary for different I—V curves from one set. To determine reasons of this alteration, all method were applied to data, which had been synthesized using one of (R_s, Φ_b, I_s, n) value differing to value calculated by using Eqs. (2–5). Some results are shown on Fig. 6.

Fig. 6(a) shows that the Gromov method R_s extraction error (i) increases with the Φ_b rise; (ii) decreases with the R_s increasing and with the I_s reduction; (iii) remains constant practically with the n changing. It is apparently, that I_s and Φ_b are connected by Eq. (2). But, in our opinion, just saturation current value, not SBH value, is a primary influencing factor for R_s determination. In favor of this assumption, there are curves 6 and 7 on Fig. 6(a). The curve 6 was obtained for I–V data set, which had been synthesized using temperature–independent values of both R_s and Φ_b. In spite of this, the χ^q_R increases with synthesis temperature rise. On the other hand, the curve 7 was obtained by using temperature–independent values of both R_s and I_s and the series resistance determination accuracy remained constant practically for whole data set. The investigation had shown that I_s and Φ_b were primary and secondary influencing factor of extraction precision respectively in the case of other parameters (not only R_s) determination and other methods (not only Gromov method) application too.

In addition, the sets of I–V data with the temperature–independent parameters were synthesized

TABLE I. The influencing factors of the Schottky diode parameters extraction. [a]

Method	Extracted parameter R_s	Φ_b	n
Norde	$n^w(\vee)$	$I_s(\downarrow)$	—
Werner	$R_s(\vee)$	$R_s(\downarrow)$, $I_s^w(\downarrow)$, $n^w(\downarrow)$	$R_s(\uparrow)$, $n^w(\downarrow)$
Werner*		$R_s(\vee)$, $I_s(\uparrow)$, $n(\uparrow)$	$R_s(\vee)$, $I_s(\uparrow)$, $n^w(\uparrow)$
Cibils	$R_s(\vee)$, $n(\uparrow)$	$R_s(\uparrow)$, $n(\vee)$	$R_s(\uparrow)$, $n(\vee)$
Cibils*		$R_s(\vee)$, $I_s(\uparrow)$, $n(\uparrow)$	$R_s(\vee)$, $I_s(\uparrow)$, $n(\uparrow)$
Kaminskii I	$R_s(\leftarrow)$, $n^w(\downarrow)$	$R_s(\vee)$, $I_s(\downarrow)$, $n(\downarrow)$	$R_s(\vee)$, $I_s^w(\downarrow)$, $n(\downarrow)$
Kaminskii* I		$R_s(\uparrow)$, $I_s(\uparrow)$, $n(\uparrow)$	$R_s(\uparrow)$, $I_s(\uparrow)$, $n(\uparrow)$
Kaminskii II	$R_s(\downarrow)$, $I_s(\rightarrow)$, $n^w(\uparrow)$	$I_s(\rightarrow)$, $n^w(\uparrow)$	$I_s(\rightarrow)$
Kaminskii* II		$I_s(\uparrow)$, $n(\uparrow)$	$I_s(\uparrow)$, $n(\uparrow)$
Bohlin	$I_s(\rightarrow)$	$I_s(\downarrow)$, $n(\wedge)$	$I_s(\rightarrow)$, $n(\wedge)$
Lee	$R_s(\downarrow)$, $I_s(\uparrow)$, $n(\uparrow)$	$I_s(\uparrow)$, $n(\uparrow)$	$I_s(\uparrow)$, $n(\uparrow)$
Gromov	$R_s(\downarrow)$, $I_s(\uparrow)$	$R_s(\uparrow)$, $I_s(\uparrow)$, $n^w(\downarrow)$	$R_s(\uparrow)$, $I_s(\uparrow)$, $n^w(\downarrow)$
Cheung	$R_s^w(\vee)$	$R_s(N)$, $I_s(\downarrow)$, $n(\downarrow)$	$R_s^w(N)$, $I_s(\rightarrow)$, $n(\downarrow)$
Mikhelashvili	$R_s(\uparrow)$, $I_s(\downarrow)$, $n^w(\downarrow)$	$R_s(\uparrow)$, $I_s(\wedge)$, $n^w(\downarrow)$	$R_s(\uparrow)$, $I_s(\wedge)$, $n^w(\downarrow)$
Ordinary LS	$R_s(\downarrow)$	$R_s(\uparrow)$, $I_s^w(\downarrow)$, $n^w(\downarrow)$	$R_s(\uparrow)$, $n^w(\downarrow)$
Lambert LS	$R_s(\downarrow)$	$I_s^w(\downarrow)$	$n^w(\downarrow)$
EAs	$R_s(\downarrow)$, $I_s^w(\uparrow)$	$R_s(\uparrow)$, $I_s(\vee)$, $n^w(\downarrow)$	$R_s(\uparrow)$, $I_s(\vee)$, $n^w(\downarrow)$

[a] The presence of R_s or I_s or n in the cell indicates the impact on extracted parameter accuracy; the subscript and inside bracket symbol deal with extraction error behavior with influencing factor increasing — see details in the text.

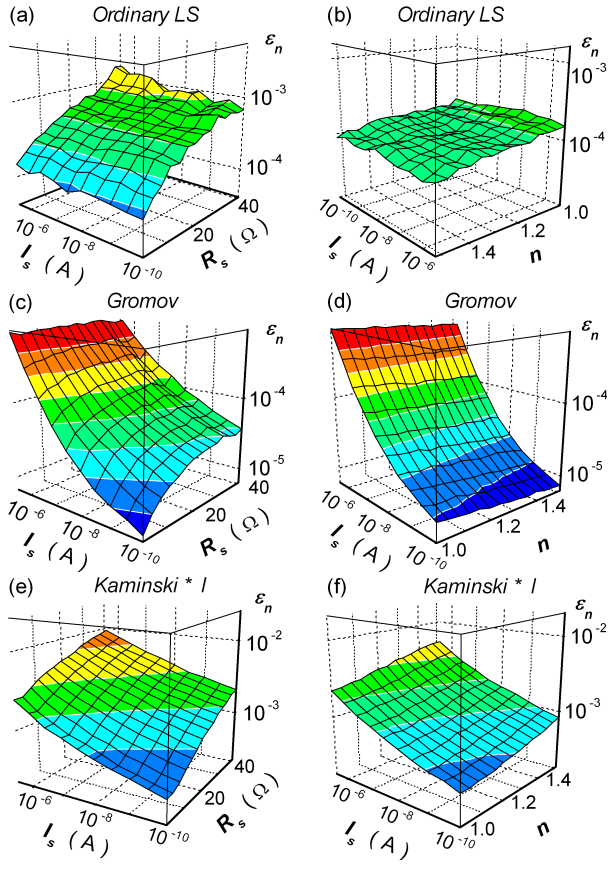

FIG. 9. Accuracy of the ideality factor extraction from data sets, which calculated using invariable value of both R_s and I_s (a, c, e) and invariable values of both n and I_s (b, d, f). The results of Ordinary LS (a, b), Gromov (c, d), and Kaminskii* I (e, f) methods are shown.

to determine influencing factors of a parameters extraction error. In this case (i) the invariable values of both R_s and I_s (or n and I_s) were used in the whole temperature range; (ii) the n (or R_s) value was calculated as aforesaid in subsection II B. From one data set to another temperature–independent R_s, n and I_s varied from 2 to 41 Ω, from 1 to 1.52 and from 10^{-10} to $5 \cdot 10^{-5}$ A respectively. Then all methods were applied to all generated data sets and parameters extraction precision was determined. Some results are shown on Figs. 7–9. So Fig. 7(a) confirms that Gromov method R_s extraction error decreases and increases with rise of R_s and I_s value respectively.

The finding about influencing factors are summarized in Table I. Some symbols are used in Table I to describe the extraction error behavior as influencing factors value is changing. If the extraction error monotonically decreases or increases with rise of influencing factor, then the symbols "↓" or "↑" are used respectively. Such as these symbols are used to characterize correlation of the Gromov method R_s extraction error and the R_s and I_s values.

It is found that extraction precision does not depend on influencing factor value monotonically only. Fig. 6(b) and Fig. 8(a) show that the Kaminskii I method Φ_b extraction error increases with series resistance rise at large R_s (> 10 Ω) and decreases at small R_s. The symbol "∨" is used in Table I to indicate such dependence. Similar dependence is observed for Chueng method R_s extraction error — see Fig. 7(d). But in this case R_s value had relatively weak effect on the R_s determination accuracy. The like weak dependences are emphasized in Table I by the subscript "w". Another examples of weak dependences on I_s and n can be seen on Figs. 7(e) and

TABLE II. Estimated running time of the parameters determination by different methods from a single I–V curve.

Method	Running time, s	
	max	min
Norde	$3.7 \cdot 10^{-5}$	$2.6 \cdot 10^{-5}$
Werner[a]	$4.5 \cdot 10^{-5}$	$4.0 \cdot 10^{-5}$
Cibils[a]	$5.3 \cdot 10^{-3}$	$1.9 \cdot 10^{-4}$
Kaminskii I[a]	$8.0 \cdot 10^{-5}$	$4.5 \cdot 10^{-5}$
Kaminskii II[a]	$2.6 \cdot 10^{-3}$	$3.0 \cdot 10^{-4}$
Bohlin	$6.3 \cdot 10^{-5}$	$4.0 \cdot 10^{-5}$
Lee	$3.6 \cdot 10^{-3}$	$1.8 \cdot 10^{-4}$
Gromov	$2.2 \cdot 10^{-2}$	$2.2 \cdot 10^{-2}$
Gromov[b]	$4.6 \cdot 10^{-5}$	$2.7 \cdot 10^{-5}$
Cheung	$3.2 \cdot 10^{-5}$	$2.0 \cdot 10^{-5}$
Mikhelashvili	$4.7 \cdot 10^{-5}$	$2.9 \cdot 10^{-5}$
Ordinary LS	460	1.8
Lambert LS	540	7.6
DE	0.73	0.36
PSO	0.35	0.14
MABC	0.20	$5.7 \cdot 10^{-2}$
TLBO	19.2	5.4

[a] The time of I–V curve correction and linear fitting is $1.8 \cdot 10^{-5}$ s (max) or $1.4 \cdot 10^{-5}$ s (min).
[b] If adaptive procedure is not used.

9(d) respectively.

If the plot of determination accuracy versus influencing factor value had maximum and no maximum (see Fig. 8(f)), then the symbol "∧" is used. The presence of peak as well as trough on a plot, e.g. Fig. 8(c), is described by the symbol "N".

Another example of dependence is shown on Fig. 7(c). The Kaminskii I method R_s extraction error remains a constant in the wide range of R_s and I_s values and increases at a small R_s value only. The similar correlation of the extraction error and influencing factor value are designated by the symbol "⌐". The symbols "¬", "⌐" are used if an extraction error increases and decreases respectively at a large influencing factor value only.

One can see that the influencing factors of both Φ_b extraction and n extraction are similar in most method cases. The use of the adaptive procedure in Gromov method of Φ_b and n determination results in the becoming of dependence on R_s value and in the damping of dependence on n value. The precision of Werner*, Cibils* and Kaminskii* methods are more susceptible to parameters value then non-asterisk ones. The most weak dependence of parameter extraction accuracy is observed in the numerical (especially Lambert LS) methods cases.

The obtained RT values are listed in Table II. The RT depends on the number of I–V curve points; therefore two values, which are obtained for I–V data generated at 130 K and 330 K, are presented in Table II. It is evident that (i) the analytical methods RT is negligibly small; (ii) in the case of I–V curve with the large number of experimental points the numerical methods RT can reach considerable value; (iii) the use of Lambert function for numerical calculation results in the RT increasing; (iv) the use of the adaptive procedure in Gromov method leads to operation time increasing, but RT don't become too much; (v) MABC and TLBO methods are most speedy and most slow respectively among used evolutionary algorithms.

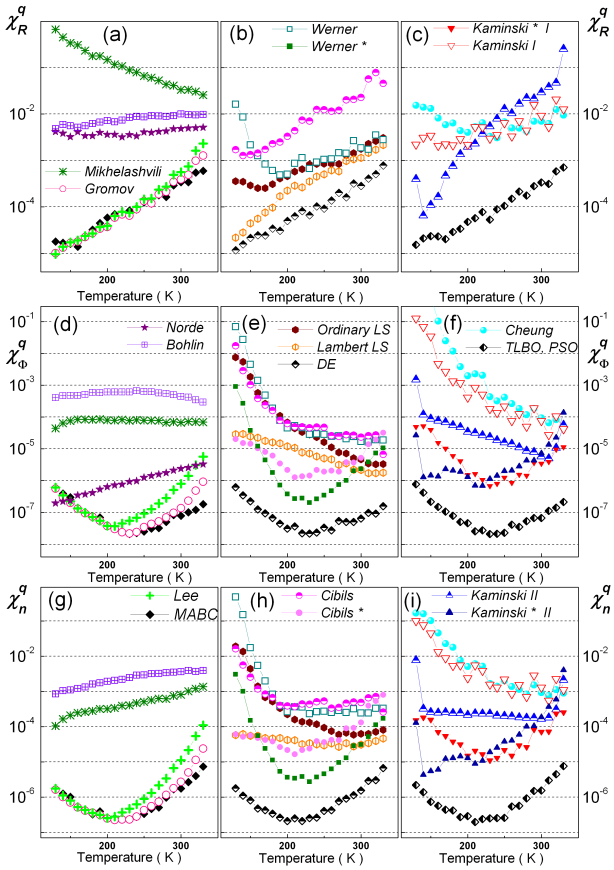

FIG. 10. Dependences of the precision of the series resistance (a – c), SBH (d – f) and ideality factor (g – i) extraction by different methods on the synthetics temperature. The set of noisy I–V curves is used. $\sigma_V = 0.3$ mV, $\sigma_I^{\varepsilon} = 1\%$.

In subsection summary, the evolutionary algorithms seem to be most reliable SD parameters extraction method due to their low error, moderate precision susceptibility to parameter value and tolerated RT. Another preferred methods are adaptive Gromov and Lambert LS. But first one determination error of the first one increases considerably when going to higher saturation currents (higher temperatures). The main imperfection of Lambert LS method is a large RT.

B. Parameter determination with noisy synthetic data

Figs. 10 and 11 show results of methods applying to some noisy data sets. Expectedly the determination error increases with a noise level rise. The dependences of accuracy extraction from single I–V curve are similar to

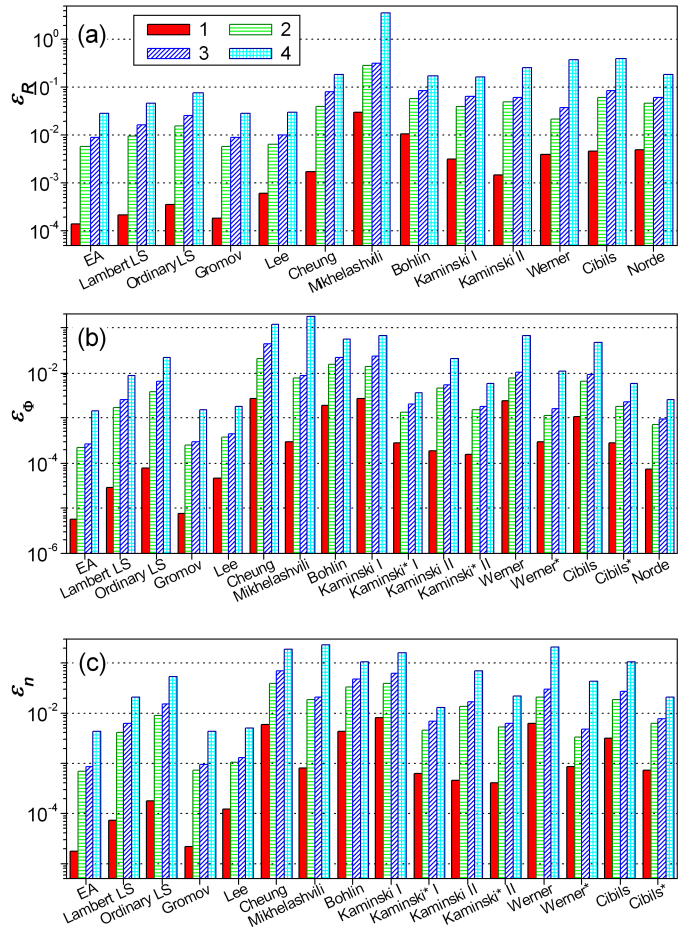

FIG. 11. Accuracy of the R_s (a), Φ_b (b) and n (c) determination from sets of noisy data. σ_V, mV: 0 (1), 0.3 (2, 3), 2 (4). σ_I^ε, %: 0 (1), 0.5 (2), 1 (3, 4).

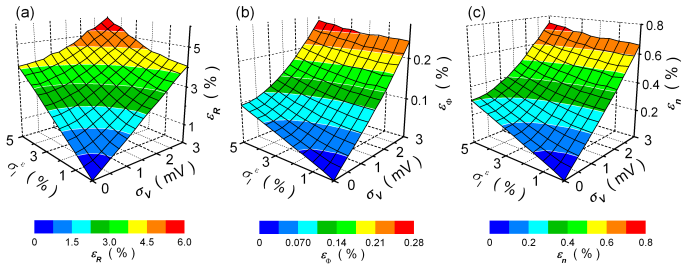

FIG. 12. Dependences of the precision of the R_s (a), Φ_b (b) and n (c) extraction by Gromov method on the the current and voltage measurement errors.

ones, which are obtained by ideal data analysis. Therefore the precision influencing factors are identical too. In addition, other features are conformable to ideal data case. So the use of Lambert function allows to achieve a more high precision of the numerical determination of SD parameters. EAs, Gromov, and Lee methods yield minimum error results. On the other hand, advantages of adaptive procedure in Gromov method are disappearing (i.e. the difference in Gromov and Lee method results is decreasing) with the noise level increasing.

If Werner, Cibils and both Kaminskii methods are applied to noisy data then n determination from corrected I–V curve is more accurate as against an auxiliary function using. Furthermore these methods error approximates to the best methods results and becomes commensurate with numerical methods accuracy or better. The Norde method yields good enough result of Φ_b extraction, but ideality factor remains undetermined.

The dependences of the parameters extraction accuracy on a noise level (or on a measurements error) are shown on Figs. 12. These plots are obtained by using Gromov method, but they are representative for the rest methods too. One can see that the dependences of extraction error on both voltage and current measurement error are close to linear. In addition, the ration of the determination error induced by voltage noise and the determination error induced by current noise is larger considerably for Φ_b and n extractions than for the R_s extraction.

C. Parameter determination with experimental data

The results of parameter determination from experimental data are shown on Fig. 13. The Bohlin method results have been obtained by using $\gamma_1 = 1.6$ and $\gamma_2 = 1.8$ because the minimum of Norde's function with $\gamma = 3.5$ was absent in the used current range.

The observable SBH dependence, which differed from Eqs.(3), can be attributed to the metal-semiconductor contact inhomogeneity.[43,44] The R_s increasing at high temperature can be account for prevalence of contact resistance.[45]

The EAs, Gromov, and Lee methods yield the similar non-monotonic temperature dependence of R_s and the slightly dissimilar value. Taking into account a small R_s value (about 1 Ω) and a considerable increasing of Gromov and Lee methods error at small R_s and big I_s values (see Figs. 5(a), 7(a), 7(b), 10(a)), we believe that values, obtained by evolutionary algorithms applying, are more correct. From the physical reason, the observed smooth parameter variation with temperature is realistic. The numerical methods yield the smooth curves R_s vs T too but the curves behavior differs at low temperature (Fig. 13(b)). On the other hand, the noisy temperature dependences should be evidence of determination or measurement errors and such curves are plotted by other method application.

The similar dependences are observed in the cases of Φ_b and n extraction too. The Φ_b value spread is smallest and it correlates with obtained smallest SBH extraction error (see Figs. 10 – 12). The worst results are observed for Bohlin, Mikhelashvili and Cheung methods.

To estimate the deviation between a measured and a fitted I–V characteristic the mean relative deviation of

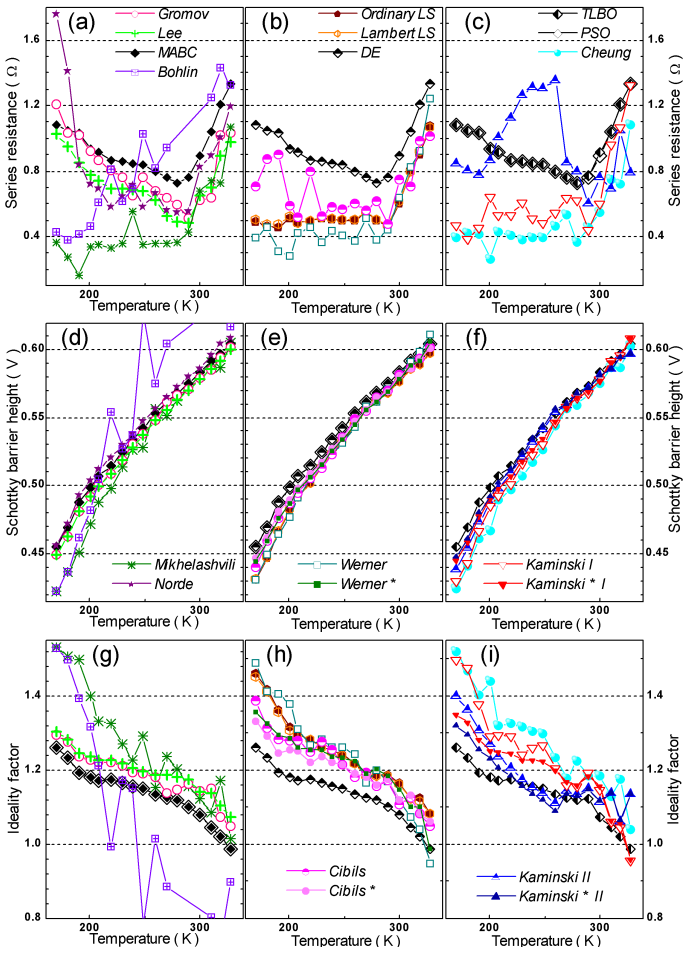

FIG. 13. Temperature dependences of R_s (a – c), Φ_b (d – f) and n (g – i) determined by different methods from experimental data.

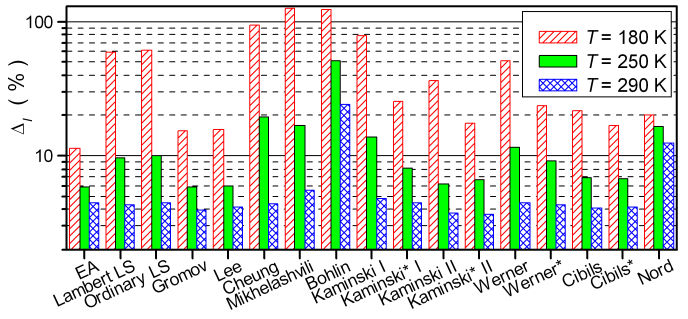

FIG. 14. Mean relative deviation of calculated current values from experimental current values.

current Δ_I was used:

$$\Delta_I = \frac{1}{N_p}\sum_{i=1}^{N_p}\left|\frac{I_{calc}(V_i) - I_i}{I_i}\right|. \qquad (63)$$

Here $I_{calc}(V_i)$ was calculated by using Eqs. (1–2) and parameters, which extracted by various method application. The results for the three I-V curves, measured at different temperatures, are presented on Fig. 14. In this case, the evolutionary algorithms, Gromov, and Lee methods show their advantage too.

V. CONCLUSION

In this work, 16 methods were implemented to extract the physical parameters of Schottky diodes. To do so, experimental and synthetic I–V data were used. It has been analyzed the dependences of extraction accuracy of series resistance, barrier height and ideality factor on the parameters value and on the noise level of the I–V curve. It has been shown that the use of Lambert function for numerical calculation allows to reduce both the determination error value and the number of accuracy influencing factor; whereas the running time increases. It has been examined the adaptive procedure, which provide selection of the I–V data range for an auxiliary function construction taking into account the deviation of calculated curve and curve under investigation. This procedure find out to improve the accuracy of analytical Gromov method, especially in the case of low noise level data. In consideration of evolutionary algorithms, the MABC method is favorable over the DE, the PSO and the TLBO due to the minimal running time. The most reliable and preferred methods seem to be evolutionary algorithms (specifically the MABC), Gromov method with adaptive procedure and Lee method. The first one is reasonable in the case of a small R_s value (a few ohms) or a large I_s value (high temperature).

This work of review, test and comparative analysis of different techniques for determination of Schottky diode parameters should be useful for further research and development on metal-semiconductor devices.

[1] E. H. Rhoderick and R. H. Williams, *Metal Semiconductor Contacts*, 2nd ed. (Clarendon Press, Oxford, 1988).
[2] S. M. Sze, *Semiconductor Devices: Physics and Technology* (Wiley, New York, 1985).
[3] H. Norde, J. Appl. Phys. **50**, 5052 (1979).
[4] C. D. Lien, F. So, and M. Nicolet, IEEE Trans. Electron Devices **ED-31**, 1502 (1984).
[5] J. H. Werner, Appl. Phys. A **47**, 291 (1988).
[6] S. Cheung and N. W. Cheung, Appl. Phys. Lett. **49**, 85 (1986).
[7] D. Gromov and V. Pugachevich, Appl. Phys. A **59**, 331 (1994).
[8] T. C. Lee, S. Fung, C. Beling, and H. Au, J. Appl. Phys. **72**, 4739 (1992).
[9] K. E. Bohlin, J. Appl. Phys. **60**, 1223 (1986).
[10] R. M. Cibils and R. H. Buitrago, J. Appl. Phys. **58**, 1075 (1985).
[11] J.-C. Manifacier, N. Brortryb, R. Ardebili, and J.-P. Charles, J. Appl. Phys. **64**, 2502 (1988).
[12] V. Mikhelashvili, G. Eisenstein, V. Garber, S. Fainleib, G. Bahir, D. Ritter, M. Orenstein, and A. Peer, J. Appl. Phys. **85**, 6873 (1999).
[13] A. Kaminski, J. Marchand, and A. Laugier, Solid-State Electron. **43**, 741 (1999).
[14] A. Ortiz-Conde, F. Garsia Sanchez, J. Liou, J. Andrian, R. Laurence, and P. Schmidt, Solid-State Electron. **38**, 265 (1995).
[15] H. Durmus and U. Atav, Appl. Phys. Lett. **99**, 093505 (2011).
[16] K. Sato and Y. Yasumura, J. Appl. Phys. **58**, 3655 (1985).

[17] M. Lyakas, R. Zaharia, and M. Eizenberg, J. Appl. Phys. **78**, 5481 (1995).
[18] A. Ortiz-Conde, Y. Ma, J. Thomson, E. Santos, J. Liou, F. Garsia Sanchez, M. Lei, J. Finol, and P. Layman, Solid-State Electron. **43**, 845 (1999).
[19] E. Evangelou, L. Papadimitriou, C. Dimitriades, and G. Giakoumakis, Solid-State Electron. **36**, 1633 (1993).
[20] D. Donoval, J. de Sousa Pires, P. Tove, and R. Harman, Solid-State Electron. **32**, 961 (1989).
[21] A. Ferhat-Hamida, Z. Ouennoughi, A. Hoffmann, and R. Weiss, Solid-State Electron. **46**, 615 (2002).
[22] W. Jung and M. Guziewicz, Materials Science and Engineering B **165**, 57 (2009).
[23] A. Ortiz-Conde and F. J. G. Sanchez, Solid-State Electron. **49**, 465 (2005).
[24] V. Aubry and F. Meyer, J. Appl. Phys. **76**, 7973 (1994).
[25] M. Ye, X. Wang, and Y. Xu, J. Appl. Phys. **105**, 094502 (2009).
[26] K. Wang and M. Ye, Solid-State Electron. **53**, 234 (2009).
[27] Y. Li, Microelectron. Eng. **84**, 260 (2007).
[28] K. Ishaque, Z. Salam, H. Taheri, and A. Shamsudin, Solar Energy **85**, 1768 (2011).
[29] S. J. Patel, A. K. Panchal, and V. Kheraj, Applied Energy **119**, 384 (2014).
[30] N. Karaboga, S. Kockanat, and H. Dogan, Appl. Intell. **38**, 279 (2013).
[31] K. Wang and M. Ye, Int. J. Mod. Phys. C **20**, 687 (2009).
[32] A. Sellai and Z. Ouennoughi, Int. J. Mod. Phys. C **16**, 1043 (2005).
[33] D. K. Schroder, *Semiconductor Material and Device Characterization*, 3rd ed. (John Wiley & Sons, New Jersey, 2006).
[34] M. Aboelfotoh, J. Appl. Phys. **66**, 262 (1989).
[35] S. Zhua, R. L. V. Meirhaeghea, C. Detaverniera, G.-P. Rub, B.-Z. Lib, and F. Cardon, Solid State Commun. **112**, 611 (1999).
[36] J. Munguia, J.-M. Bluet, O. Marty, G. Bremond, M. Mermoux, and D. Rouchon, Appl. Phys. Lett. **100**, 102107 (2012).
[37] T. C. Lee, T. P. Chen, H. L. Au, S. Fung, and C. D. Beling, Phys. Stat. Sol. (a) **152**, 563 (1995).
[38] P. G. McCafferty, A. Sellai, P. Dawson, and H. Elabd, Solid-State Electron. **39**, 583 (1996).
[39] A. Saxena, Surf. Sci. **13**, 151 (1969).
[40] D. S. Meyaard, J. Cho, E. F. Schubert, S.-H. Han, M.-H. Kim, and C. Sone, Appl. Phys. Lett. **103**, 121103 (2013).
[41] W. P. Kang, J. L. Davidson, Y. Gurbuz, and D. V. Kerns, J. Appl. Phys. **78**, 1101 (1995).
[42] O. Dermircioglu, S. Karatas, N. Yildirim, and O. Bakkaloglu, Microelectron. Eng. **88**, 2997 (2011).
[43] R. T. Tung, Mater. Sci. Eng., R **35**, 1 (2001).
[44] O. Y. Olikh, IEEE Trans. Nucl. Sci. **60**, 394 (2013).
[45] I. Dokme and S. Altindal, Semicond. Sci. Technol. **21**, 1053 (2006).